

# Numerical investigation of out-of-plane sound propagation in a shallow water experiment

Frédéric Sturm

*LMFA UMR CNRS 5509, Ecole Centrale de Lyon, 36, avenue Guy de Collongue, 69134 Ecully Cedex, France  
frederic.sturm@ec-lyon.fr*

Sven Ivansson

*Swedish Defence Research Agency, SE-16490 Stockholm, Sweden  
sveni@foi.se*

Yong-Min Jiang and N. Ross Chapman

*School of Earth and Ocean Sciences, University of Victoria, Victoria, BC, Canada, V8W 3P6  
minj@uvic.ca, chapman@uvic.ca*

**Abstract:** In an experiment in the Florida Straits, broadband pulses were transmitted over a range of 10 km and received by a vertical hydrophone array. For pulses with center frequency below 400 Hz, the received signal consisted of a dominant arrival followed by a secondary one delayed by about 0.4 s. A hypothesis that the secondary arrival was caused by 3D out-of-plane propagation is investigated here numerically with a 3D parabolic equation model (3DWAPE) and a 3D ray model (MOC3D). Both models clearly predict a secondary arrival caused by 3D horizontal refraction from the sloping bottom in the shoreward direction.

© 2008 Acoustical Society of America

**PACS numbers:** 43.30.Bp, 43.30.Dr, 43.30.Cq [GD]

**Date Received:** July 30, 2008      **Date Accepted:** September 30, 2008

## 1. Introduction

Results from an inversion to estimate geoacoustic bottom parameters using broadband data from an experiment in the Florida Straits have recently been reported by Jiang *et al.*<sup>1</sup> M-sequence sound pulses were transmitted over a range of 10 km and received by a vertical hydrophone array. For the sound pulses whose center frequency was lower than 400 Hz, the received signal consisted of a dominant first arrival followed by a secondary component delayed by about 0.4 s in arrival time. Initial inversions using conventional matched-field inversion methods that assumed the second arrival was due to the sub-bottom structure were not successful. Although many different geoacoustic models were tested, from simple half-spaces to multiple layers, with and without shear parameters, none of the models was able to account for the secondary arrival. Examination using a beamforming algorithm showed that the secondary arrival was received at higher angles compared to the first one. This result suggested that the secondary arrival could be explained by horizontal refraction due to the interaction with a steeply sloping ocean bottom closer to the shore, a well known 3D propagation effect.<sup>2</sup> Successful inversions were then obtained by spatially filtering out the secondary arrival and modeling the first arrival in the 2D plane.

After some experimental and environmental information in Sec. 2, this Letter presents a numerical investigation of the 3D propagation hypothesis. A 3D parabolic equation (PE)-based model (3DWAPE) is applied in Sec. 3, and a 3D ray model (MOC3D) in Sec. 4. Both models clearly predict a secondary arrival caused by 3D horizontal refraction from the sloping bottom that steepens in the shoreward direction. Efforts to further improve the fit between modeled and measured signals are discussed in Sec. 5.

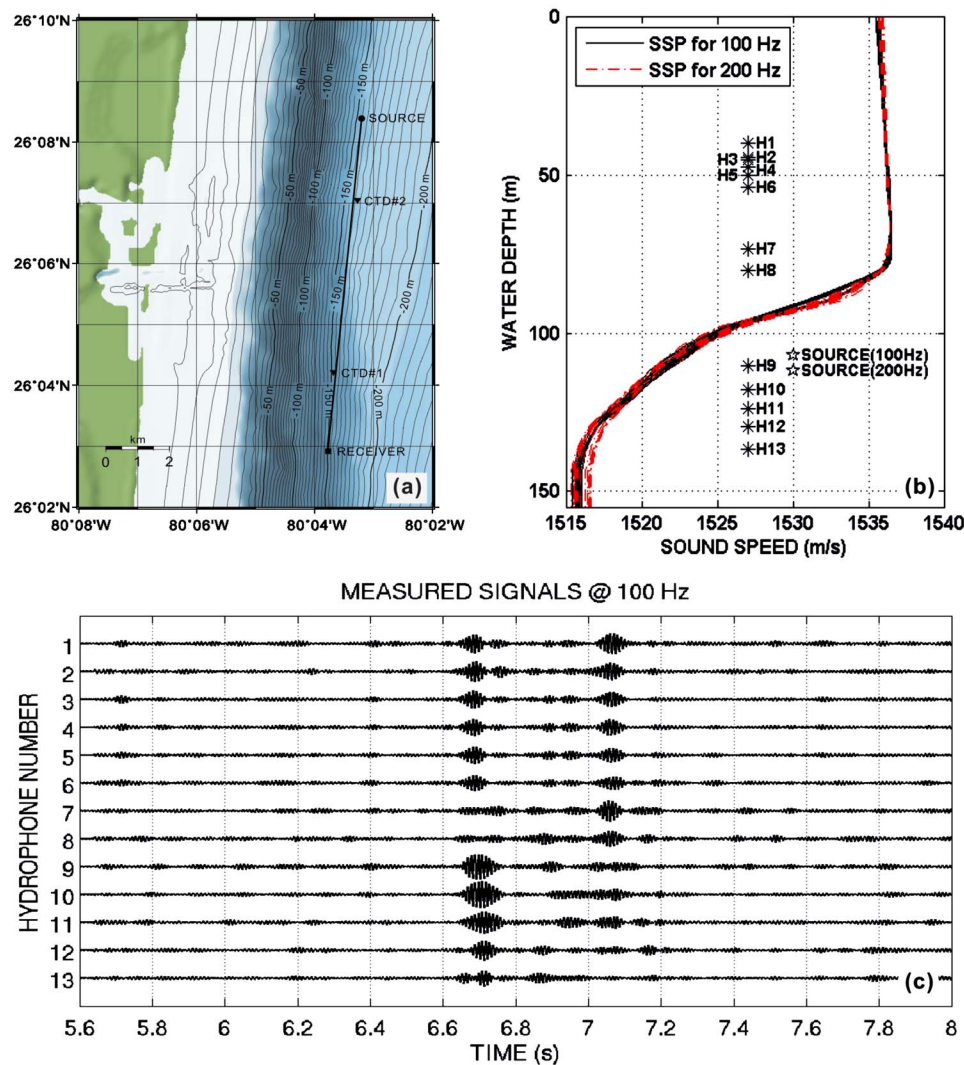


Fig. 1. (Color online) (a) experimental site and geometric setup, showing the steep portion of the bottom slope about 1.4 km west of the experimental site. The depth contours are 5 m apart; (b) sound-speed profiles of two consecutive hours. The profiles consist of an isospeed layer in the upper 80 m of the water column, followed by a strong negative gradient profile; (c) measured 100-Hz bandlimited impulse response signals at the 13 different hydrophones.

## 2. Description of the experiment

The data were collected at the South Florida Ocean Measurement Center during an acoustic propagation experiment at 10-km range in December, 1999.<sup>3</sup> Figure 1(a) is a sketch of the experimental site and the geometric setup of the measurement system. The source and vertical line array were deployed on the elevation contours of 155 and 150 m, respectively. Two environmental arrays (black triangles) were placed between the source and the array. The experimental setup was designed to study sound propagation along the shore.

The vertical line array (VLA) used in this analysis consists of 13 of the array hydrophones, unevenly spaced on the array with the shallowest at a depth of 39.8 m and the deepest at 136.7 m [see Fig. 1(b)]. The sources were at 107 m (100 Hz) and 112 m (all other frequencies). The hydrophones and low-frequency sources had broad directivities, horizontally as well as

vertically. Typical sound-speed profiles (SSPs) during the collection of the acoustic data analyzed in this paper are shown in Fig. 1(b). They were derived from the conductivity, temperature, and depth data collected by the two environmental arrays. The high correlation between these array data, and the stability in time of the SSP, support an assumption of range-independent SSP in the source-receiver plane. M-sequence coded pulses at center frequencies of 100, 200, 400, 800, 1600, and 3200 Hz were transmitted sequentially for 1 h at each frequency. The received signals were ensemble averaged over 1 min, and then compressed to get bandlimited impulse responses.

The data shown in Fig. 1(c) are the measured 100-Hz bandlimited impulse responses at the receiver depths. Notable features are (1) a second distinct group of arrivals appears at some of the hydrophones approximately 0.4 s later than the first group of arrivals; and (2) for the shallowest hydrophones, the amplitude of the second arrival is stronger than the first one. The second group of arrivals was observed experimentally in the 200- and 400-Hz data as well. However, the strength of the later arrivals decreased when frequency increased, and was negligible at frequencies greater than 800 Hz. The later arrivals at 100 Hz are the focus of attention in this Letter.

### 3. Comparisons with 3DWAPE

The numerical model 3DWAPE (Ref. 4) is an acoustic parabolic equation-based model which solves the problem of acoustic waves emanating from an isotropic (omnidirectional) point source and propagating in general 3D oceanic environments. The time dependence of the source can be either transient (broadband) or harmonic (cw). Computations with 3DWAPE were performed assuming the 100-Hz SSP in Fig. 1(b) throughout the waveguide. Bottom depths for the computation domain were obtained by bilinear interpolation on a rectangular grid of the bathymetry data.<sup>5</sup> The grid size of the bathymetry is equal to 3', i.e., approximately 83.2 m in longitude and 92.66 m in latitude in this region. In the vertical plane containing the source and the VLA, the water depth varies between 150 and 160 m. The time dependence of the source is modeled by a Gaussian-weighted cosine pulse with bandwidth 50 Hz, covering the band 75–125 Hz, and pulse length approximately 0.12 s. The omnidirectional point source was positioned at a depth of 107 m as suggested by the experiment. In the 2D (i.e., azimuthally uncoupled) and fully 3D computations, a lossy half-space fluid sediment bottom was considered with a (compressional) wave speed of 1676 m/s, a density of 1.779 g/cm<sup>3</sup>, and an attenuation of 0.05 dB per wavelength, leading to 8–9 proper modes in an approximately 155-m-deep water column.

The computed received signals on the 13 unevenly spaced hydrophones are displayed in the top two panels of Fig. 2. For comparison, the envelopes of the experimentally measured signals displayed in Fig. 1(c) are plotted as gray traces in both panels. In addition, to help understand the depth variation of the signal, the two bottom panels of Fig. 2 display the simulated time series versus depth with a very fine resolution (every 2 m in depth), thus giving evidence of modal structures of the received signals. Several observations can be made by comparing the 2D and 3D numerical predictions. The onset (around 6.7 s) of the received signals is weakly affected by 3D effects. These first arrivals correspond to time arrivals of mode 1 up to mode 4. It can be verified that both mode 5 and mode 8 are weakly excited at the source. As a result, they are absent or strongly attenuated at the vertical receiver array. The 2D and 3D late arrivals are clearly different. These arrivals correspond to time arrivals of modes 6 and 7. The 3D modal arrivals are shifted in time. This shift can explain the second group of strong arrivals around 0.45 s after the first group of strong arrivals, which is consistent with the observation from the experimental data. However, these second arrivals are strong for all depths, even below the thermocline where they are weaker in the experimental data.

### 4. Comparisons with MOC3D

Albeit less reliable, ray modeling is useful as a complement to the computer intensive 3D PE modeling. Methods which avoid the demanding 3D eigenray problem are particularly attractive. In an approach by Piskarev,<sup>6</sup> the emitted energy from the source is viewed as confined to the thin

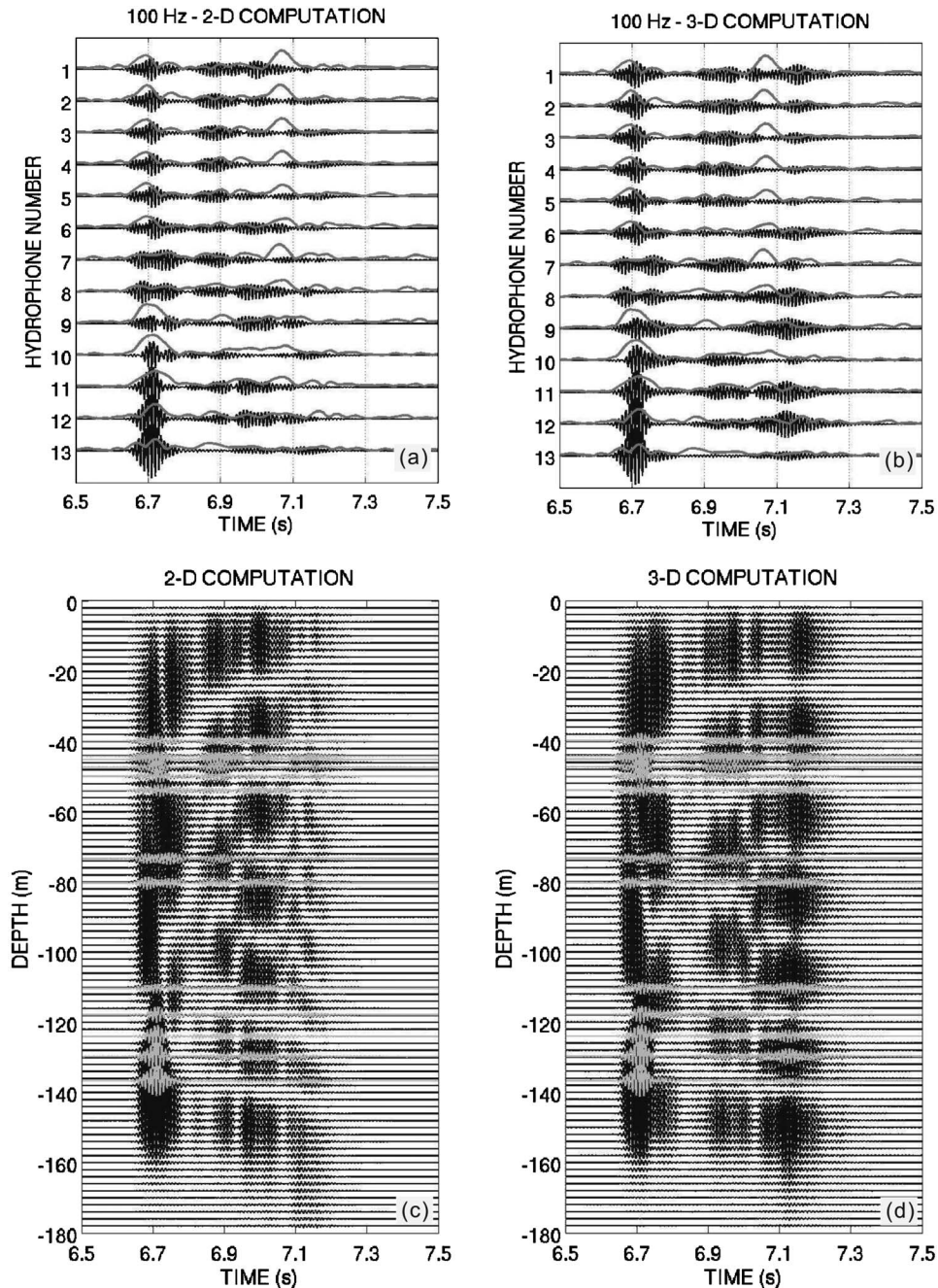


Fig. 2. Simulated time series versus hydrophone number obtained using 2D (a) and 3D (b) PE computations with 3DWAPE. The gray traces show the envelopes of the corresponding experimental data. Simulated time series versus depth obtained using 2D (c) and 3D (d) PE computations with 3DWAPE. The gray traces correspond to the simulated signals received on the 13 hydrophones.

rays, and intensities are determined as probe volume averages using the ray density. Schneider's model MOCASSIN (Ref. 7) is a 2D ray model for transmission loss and reverberation based on similar ideas. It has been taken as a starting point for developing the 3D model MOC3D,<sup>8</sup> including simulation of time series envelopes by positioning ray intensities along a time axis. The



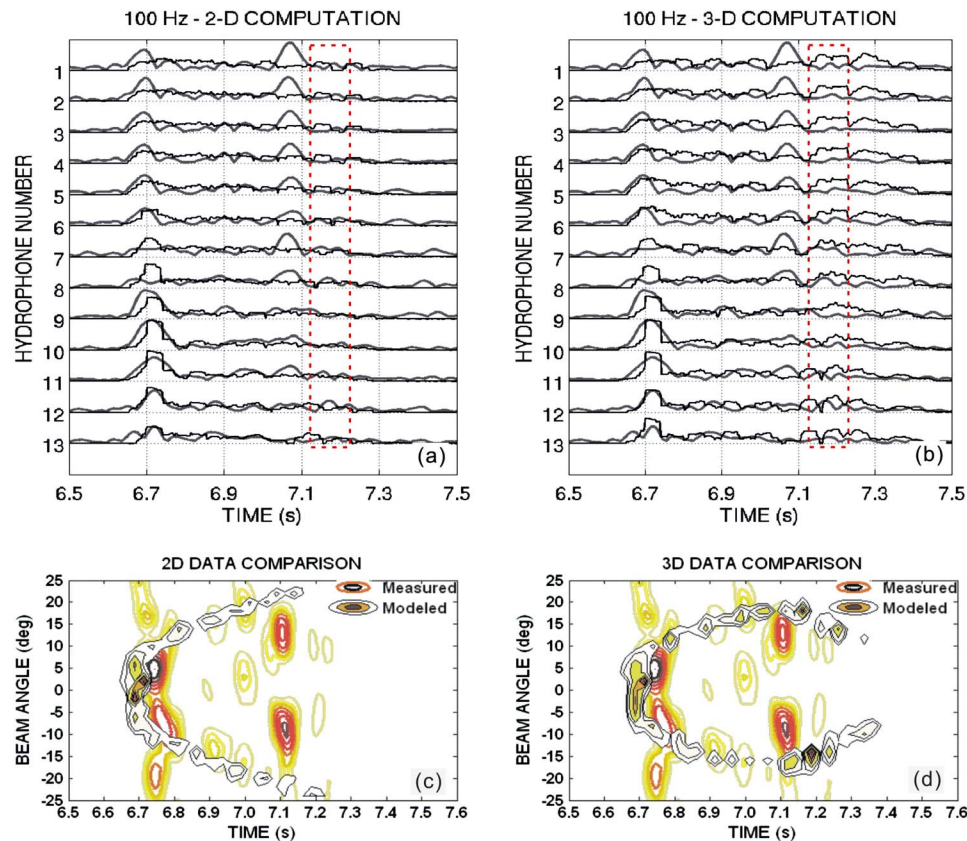


Fig. 3. (Color online) Simulated time series envelopes versus hydrophone number obtained using 2D (a) and 3D (b) computations with MOC3D. The gray traces show the corresponding experimental data. Measured vertical directionality at the array, 100-Hz case, together with ray arrival energy contours for the 2D (c) and 3D (d) MOC3D results.

ray models may be applicable down to frequencies corresponding to wavelengths of about one-tenth of the water depth. For the Florida Straits case, with the coastal slope from depths of about 155 m in the source-receiver section, results for 400 and perhaps 200 Hz may be justified. However, the applicability to low frequencies is improved by a frequency-dependent smoothing of the sound-speed profiles.<sup>7</sup>

Figures 3(a) and 3(b) show numerical results obtained with MOC3D for the 100-Hz frequency and the 13 unevenly spaced hydrophones. Following the initial arrival at about 6.7 s, and some intermediate arrivals, clear 3D effects appear at about 7.15 s in the model traces. As verified by ray path plots and travel-time/back-azimuth diagrams, the corresponding arrivals are caused by horizontal refraction from the sloping bottom. Indeed, as the ray travel times increase from 7.1 to 7.3 s in the 3D computation, the ray back-azimuths at the array decrease from about  $-10^\circ$  to about  $-20^\circ$ . The source is at about  $+5^\circ$  from north at  $0^\circ$  [see Fig. 1(a)] and 3D propagation out of the vertical source-receiver plane has clearly taken place. As in the 3DWAPE solutions in Fig. 2, the time delay (about 0.45 s) is somewhat larger than in the measured data (about 0.4 s), and the 3D effects are clearly seen also below the thermocline.

The vertical arrival structure of the measured data obtained by beamforming<sup>1</sup> is shown in Figs. 3(c) and 3(d), together with energy contours for the MOC3D ray arrivals as positioned in time and vertical angle. The 3D modeling produces highlights in the travel-time/beam-angle plane with an improved fit to the measured data, as compared to the 2D modeling.

## 5. Discussion and Conclusion

The results from this investigation provide support for the 3D propagation hypothesis used by Jiang *et al.* in their inversion of the Florida Straits data. Both numerical propagation models predict a secondary arrival caused by 3D horizontal refraction from the sloping bottom that steepens closer to the shore. The modeled and measured delay times and the vertical directionality of the signal agree reasonably well, given the lack of information about the sound-speed variation in the water column over the 3D grid. Other ray simulations (not shown here) showed that the amplitude reduction of the secondary arrival at higher frequencies can be modeled by introducing a 1-m-thick sediment layer (wavespeed 1500 m/s, density 1.2 g/cm<sup>3</sup>, attenuation 0.4 dB per wavelength) on top of the bottom half-space. The effect of this additional thin sediment layer on the secondary arrival is very small in the 100-Hz case. It is worth mentioning that further adaptations of the environmental parameters can improve the fit to the 100-Hz measurement data, for example, by increasing the sound speed in the water column and making the bottom half-space (below the 1-m-thick sediment layer) harder as the bottom depth decreases in the shoreward direction. Overall, the investigation shows that 3D propagation should not be ignored in interpretation of data from shallow-water environments, particularly in long-range, along shelf propagation geometries.

## Acknowledgments

Support from Office of Naval Research Ocean Acoustics Team is acknowledged by Y-M.J. and N.R.C.

## References and links

- <sup>1</sup>Y. Jiang, N. R. Chapman, and H. A. DeFerrari, "Geoacoustic inversion of broadband data by matched beam processing," *J. Acoust. Soc. Am.* **119**, 3707–3716 (2006).
- <sup>2</sup>A. Tolstoy, "3-D propagation issues and models," *J. Comput. Acoust.* **4**, 243–271 (1996).
- <sup>3</sup>H. B. Nguyen, H. A. DeFerrari, and N. J. Williams, "Ocean acoustic sensor installation at the South Florida ocean Measurement Center," *IEEE J. Ocean. Eng.* **27**, 235–244 (2002).
- <sup>4</sup>F. Sturm, "Numerical study of broadband sound pulse propagation in three-dimensional oceanic waveguides," *J. Acoust. Soc. Am.* **117**, 1058–1079 (2005).
- <sup>5</sup>GEODAS Search and Data Retrieval Systems, National Geophysical Data Center (NGDC) ([http://www.ngdc.noaa.gov/mgg/gdas/gd\\_designagrid.html](http://www.ngdc.noaa.gov/mgg/gdas/gd_designagrid.html)) Last viewed 11/2006.
- <sup>6</sup>A. L. Piskarev, "Calculation of the average intensity distributions of sound fields in the ocean," *Sov. Phys. Acoust.* **35**, 418–422 (1989).
- <sup>7</sup>H. G. Schneider, "MOCASSIN sound propagation and sonar range prediction model for shallow water environments," User's guide, Technical Report 1990-9, FWG, Kiel, Germany (1990).
- <sup>8</sup>S. Ivansson, "Stochastic ray-trace computations of transmission loss and reverberation in 3-D range-dependent environments," in *Proceedings of the 8th ECUA, Portugal, 2006*, pp. 131–136.